Ion formation and kinetic electron emission during the impact of slow atomic metal particles on metal surfaces

Z. Sroubek,[1,2] X. Chen,[1] and J. A. Yarmoff[1,*]

[1]*Department of Physics, University of California, Riverside, California 92521, USA*
[2]*Czech Academy of Sciences, URE, Chaberska 57, Prague 8, Czech Republic*

The charge distributions of slow atomic particles that are singly scattered, multiply scattered, recoiled, and sputtered from metal surfaces are analyzed in terms of both nonadiabatic particle-substrate electron transfer and electron transfer from electronically excited substrates. The results are compared to experimental data for 50 eV Na^+ ions scattered from Cu(001), and Al atoms sputtered and recoiled from Al(100). The comparison allows for a quantitative determination of the role of substrate excitations in surface charge exchange. In addition, an analysis of kinetic electron emission (KEE) is carried out using similar low-energy metal projectile-metal substrate systems. Contributions to KEE from various nonadiabatic processes are quantitatively evaluated, including the same process that is responsible for charge formation in single-scattering experiments. The results are compared to experimental KEE data induced by Na^+ impinging on Ru(0001). The contributions of nonadiabatic one-electron processes are shown to be small when realistic particle-substrate parameters are used. Many-electron interactions are assumed to play an important role in explaining KEE and, as an illustration, a simplified hot-spot model is outlined.

I. INTRODUCTION

Ionization and neutralization of metal atoms emitted from solid surfaces by the impact of atomic projectiles is an important process leading to the formation of ions in scattering, recoiling, and sputtering experiments. An understanding of the processes involved is not only of intrinsic interest, but is essential for the interpretation of analytical techniques such as ion scattering spectroscopy (ISS), direct recoil spectroscopy (DRS), and secondary ion mass spectrometry (SIMS).

When an atomic metal particle is emitted from a solid surface, it may be positively charged if an electron is transferred from the projectile to the metal, or negatively charged if an electron from the metal is transferred to the projectile. This paper deals with very slow particles having hyperthermal energies so that the electron transfer involves the valence electron bands close to the Fermi energy. Thus, any deep level promotions and deep hole excitations are excluded. The process of transferring valence electrons from an undisturbed metal to the projectile is nonadiabatic because of the energy deficit, represented by the energy difference between the ionization or affinity level of the projectile and the Fermi level. This deficit must be overcome by a quantum mechanical transition induced by the motion of the particle. Typically, the probability of the transfer is proportional to $\exp(-b \cdot \delta\varepsilon / v)$, where $\delta\varepsilon$ is the energy deficit, v is the velocity of the particle, and b is a constant. The process usually depends significantly on v. However, when the metal substrate in the near-surface region is electronically excited, i.e., it contains electrons above and holes below the Fermi level, some of these excitations can be transferred to the emitted particle without the need to overcome the energy deficit. The ionization process is then far less velocity dependent and is basically adiabatic. It is the purpose of this paper to discuss the experimental evidence and the theoretical justification of these two processes using experimental data collected from well-defined metallic systems.

Similar processes as those involved in ion formation may, in principle, be encountered in kinetic electron emission (KEE) induced by the impact of atomic metal projectiles with metallic surfaces. The particles are again assumed to be slow enough to avoid the promotion of deep levels in the substrate and projectile. In such a case, formally similar matrix elements between the particle and the substrate valence band can cause both nonadiabatic ion formation and electron emission. The time scale of KEE is very short, typically a few fs, and any contribution of adiabatic processes is therefore unlikely. The similarities and differences between ion formation and electron emission are discussed in this paper, and the specific features of KEE are identified.

Section II A presents the nonadiabatic model of ionization and neutralization. This process is important for ion formation during single scattering and direct recoiling. Good agreement with experiment is obtained when the metallic substrate is described by the jellium model. Deviations from this simple nonadiabatic one-electron picture are observed, however, when the particle is multiply scattered or sputtered from the metal. The problem is conceptually more complicated, as the experiments show that collisional perturbation of the substrate, prior to the particle emission, clearly influences the charge state of the emitted particle. A simplified model is described in which the charge transfer is changed by quasistatic charges induced by the substrate surface perturbations. In Sec. II B, a second, more realistic, model is outlined in which the charge transfer is changed by electron-hole (e-h) excitations induced by the motion of substrate atoms. In Sec. III A, KEE is described in terms of a one-electron nonadiabatic process produced by the motion of the bombarding particle through the jellium electron gas. The perturbing particle is described by various model potentials,

including the one responsible for the particle charge formation outlined in Sec. II A. In Sec. III B, a possible extension of one-electron models of KEE is discussed using a simplified hot-spot model.

II. ATOMIC PARTICLES SCATTERED AND SPUTTERED FROM METALLIC SURFACES

A. Nonadiabatic models of ionization and neutralization

There is extensive experimental and theoretical evidence that ion formation and neutralization during the single scattering of slow atomic metal particles from metal surfaces is a purely nonadiabatic process.[1–3] As mentioned above, the energy of the impinging particle is assumed to be sufficiently small so that only valence electrons are involved in the process. Currently, the only existing manageable mathematical formalism that can handle the complex mechanism of ion formation by transfer of electrons to and from the valence band is the Anderson-Newns Hamiltonian.[4–6] Although the model based on this Hamiltonian is parametrical and consequently does not provide a quantitative estimate from first principles, its simplicity allows for dynamical solutions to be obtained. A more precise approach is a time-independent ground-state model, in particular one based on density functional theory. Although this cannot be used for dynamical studies, it has been used successfully to obtain values for some of the parameters of the Anderson-Newns Hamiltonian.[7,8] The most appropriate description of the dynamical processes would be in terms of time-dependent density functional theory,[9] but the apparent complexity of this approach still hinders its application in the analysis of ion formation.

The parameters in the Anderson-Newns Hamiltonian that are relevant for ion formation processes at the surface[4–6] are the virtual line width $\Delta(z)$ of the ionization (or affinity) level of the emitted particle and the energy separation $\delta\varepsilon(z)$ between the Fermi level of the metal surface and the ionization (or affinity) level of the atom. Both parameters are functions of the particle's distance z from the surface. When the particle is moving, the distance z is a function of time $z(t)$ and the Hamiltonian becomes time dependent. The solution can be sought in terms of a linear combination of many-electron configurations[6] or in terms of an independent-electron framework.[4,5] The latter approach is sufficiently precise for most applications, and it leads, in the infinite valence-band width approximation, to the following compact formula for the neutralization probability N_p (note that atomic units are used in this paper unless stated otherwise):

$$N_p = (1/\pi) \int d\varepsilon \cdot f(\varepsilon, T_e) \left| \int_{-\infty}^{+\infty} [\Delta(t')/2]^{1/2} \right.$$
$$\left. \times \exp\left\{ -i\varepsilon t' - \int_{t'}^{\infty} [i\delta\varepsilon(t'') + \Delta(t'')/2]dt'' \right\} dt' \right|^2 . \tag{1}$$

The metallic substrate is typically (and also in our case) represented by the jellium model, and Eq. (1), with $\Delta(z)$ and

$\delta\varepsilon(z)$ calculated with the use of the density functional formalism or other well-established methods, is known to give reasonable agreement with low energy ion scattering experiments. Equation (1) also contains the electronic temperature T_e as an additional parameter which describes a possible smearing of the Fermi level of the substrate, and $f(\varepsilon, T_e)$, which is the corresponding Fermi distribution with the Fermi energy set to zero. At large z, the z dependence of the energy $\delta\varepsilon(z)$ is most often described by the image potential and $\Delta(z)$ is proportional to $\exp(-2\gamma z)$, where γ is the inverse length of the atom-surface interaction. Appropriate analytical expressions for $\delta\varepsilon(z)$ and $\Delta(z)$,[6,10] which are also used in this paper, are

$$\delta\varepsilon(z) = \phi - I + (16z^2 + 109.44)^{-1/2}, \tag{2}$$

where I is the ionization energy of the atom, ϕ is the surface work function of the substrate, and the last term is the saturated image charge contribution. The expression for $\Delta(z)$ is

$$\Delta(z) = \Delta_0[\exp(8\gamma z) + (\Delta_0/\Delta_{sat})^4 - 1]^{-1/4}, \tag{3}$$

where Δ_0 and Δ_{sat} are constants.

To establish the general validity of Eq. (1), it is useful to study N_p as a function of the velocity of the escaping particle. In most cases studied, N_p depends only upon the perpendicular component $v_\perp$ of the velocity, and thus $z = v_\perp t$. (Although the value of $v_\perp$ changes during the emission process, the quoted $v_\perp$ refers to the final escape velocity.) The system studied by ion scattering so far over the largest range of $v_\perp$ is Na$^+$ scattered from Cu(001).[6,11] The neutralization probability N_p of Na$^+$ in single scattering was measured from $v_\perp = 0.0015$ to 0.025 a.u., and is well described quantitatively by Eq. (1) with $\gamma = 0.49$, $\Delta_0 = 1.77$, and $\Delta_{sat} = 0.073$ in Eqs. (2) and (3). The value of N_p is rather low, about 0.1 at the lowest $v_\perp$, with a broad minimum at about $v_\perp = 0.01$, and increases again with the velocity to an N_p slightly above 0.1. This behavior is fully in accord with the nonadiabatic model. It is interesting, however, that Na$^+$ scattered by more complicated trajectories can have much higher N_p even if they have the same perpendicular velocity, which is contrary to the expectation that the nonadiabatic neutralization depends only upon $v_\perp$. This point is very nicely illustrated and discussed in detail in Ref. 11, where several trajectories of scattered Na$^+$ have been precisely identified.

We have plotted two of these Na trajectories in Figs. 1 and 2, together with the trajectories of the substrate Cu atoms. The trajectories were calculated by solving the set of classical equations of motion of atoms using MATLAB 7 subroutines. The interatomic potentials used were the Molière and Morse potentials[12] and the repulsive Ne-Cu potential,[12] for Cu-Cu and Na$^+$-Cu interactions, respectively. As Na is in the charged state most of the time, the interaction with the image charge above the metal surface must be included, and was described by the saturated image potential.[6] The Cu substrate was represented by a cluster of 308 Cu atoms, roughly $20 \times 20 \times 20$ a.u.^{3} in size, with the Cu(001) surface at the top.
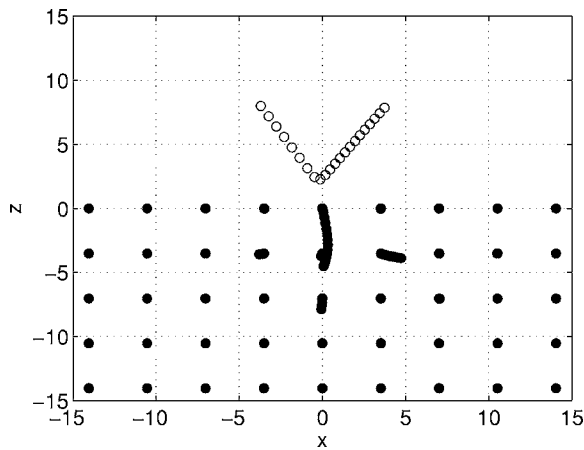
FIG. 1. Snapshot of a particular trajectory that occurs when 50 eV Na^+ impinges upon Cu(001) along the $\langle 100 \rangle$ azimuth at an impact angle of 30°. This trajectory leads to single scattering of Na from the Cu surface into an escape angle of 35°. The Na projectile is indicated by the open circles, while the trajectories of Cu atoms are marked by solid circles. The trajectory is followed up to the time when Na^+ becomes neutralized. The difference in time between each circle is 100 a.u. (2.4 fs).

As in Ref. 11 the 50 eV Na^+ ion impinges upon the Cu(001) surface along the $\langle 100 \rangle$ azimuth (the x axis), with an impact angle of 30 ° and an exit angle of 35 ° with respect to the normal (the z axis). The single-scattering trajectory shown in Fig. 1 is equivalent to the trajectory in Fig. 2(a) of Ref. 11. The escape energy of Na is 15.4 eV, which corresponds to $v_\perp = 0.0045$ a.u., and the experimental neutral fraction is below 0.07, in agreement with the prediction based on Eq. (1).

The multiple-scattering trajectory shown in Fig. 2 is equivalent to Fig. 2(f) in Ref. 11. The escape energy of Na in this case is 3 eV, which corresponds to $v_\perp = 0.002$ a.u. and the experimental neutral fraction is 0.4, i.e., seven times
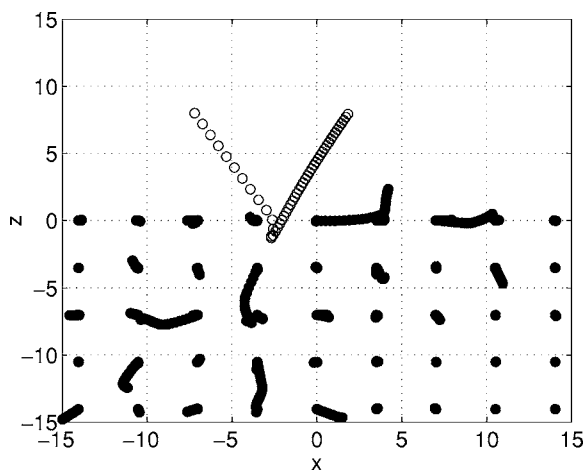
FIG. 2. Snapshot of a trajectory that occurs when 50 eV Na^+ impinges upon Cu(001) such that the Na is multiply scattered. The situation is the same as in Fig. 1, but the impact coordinates were chosen so that Na penetrates deeper in Cu before being emitted. The time between circles is again 100 a.u., and the trajectory is shown until the Na^+ ion is neutralized.

more than predicted by Eq. (1) for the unperturbed substrate. The plausible explanation is that, in the second case, the substrate is severely disturbed and the surface electronic structure strongly deviates from that of a smooth jellium surface.

To demonstrate the effect of this perturbation, snapshots of the positions of Cu and Na atoms at the time of Na neutralization are shown in Figs. 1 and 2. The most probable distance at which neutralization occurs, z_c, is estimated from Eq. (1) (or approximately from $z_c = (1/2\gamma)[\ln(\Delta_0/2\gamma v)]$ to be about $z_c = 7$–8 a.u. for both cases. The dots in the figures correspond to a time interval of 100 a.u., i.e., 2.41 fs. The time interval between the moments when the Na touches the surface at $z = 2$ a.u. and reaches z_c is 1000 a.u. (24 fs) in the single-scattering process shown in Fig. 1, and 4200 a.u. (101 fs) in the multiple-scattering process of Fig. 2.

Clearly, the surface is strongly perturbed in both cases. In Fig. 1, the Cu atom moves about 4 a.u. in the $-z$ direction whereas in Fig. 2, the Cu atom moves roughly the same distance in the x,z direction. Vacancies left when atoms are missing from the surface could be slightly negatively charged, whereas adatoms could be positively charged. These induced local charges are screened and form local dipoles with typical moments of about 0.5–1 D. Such a charge imbalance increases the potential at z_c in Fig. 2 by 0.1 eV, so that the value of N_p, as calculated from Eq. (1), would increase to $N_p = 0.386$ in agreement with the experiment. In the single-scattering trajectory shown in Fig. 1, the vacancy would cause a potential change of a similar size but of an opposite sign. The value of N_p would then be 0.01, which is a significant change. However, no effects of a charge imbalance have ever been discerned in single-scattering experiments.

Several attempts have been made to calculate the charge imbalance at the surface from first principles but precise values are difficult to obtain. Generally, the local quasistatic charges at the surface are small because of the heavy screening by the metal electrons, but random induced dipoles may be formed. As discussed above, these dipoles could explain the increase of the neutralization of Na multiply scattered from Cu because the ionization energy level of Na is very close to the Fermi level of Cu. However, similar effects, i.e., a strong enhancement of the charge exchange for more complicated trajectories of escaping atoms, have been commonly encountered in sputtering and also occur for atoms with much larger ionization energies (e.g., Al, Cu, Ag). It should be stressed that multiply scattered and sputtered atoms can be emitted at about the same time after the impact of the primary particle and they are exposed to the same excitations in the substrate.

We will show, using the example of Al sputtered from Al metal, that the surface charge imbalance would have to be very large in order to explain the observed charge exchange enhancement in atoms with larger ionization energies. Al ions scattered, recoiled, and sputtered from Al metal were studied in detail in Ref. 13. Because of the large ionization energy (6 eV), most of the emitted atoms are neutral and it is more appropriate to describe the charge exchange process in terms of the ionization probability $P^+ = 1 - N_p$. The value of P^+ can be calculated from Eq. (1), but for our purpose it is

suitable to use an approximation of Eq. (1) for very small perpendicular velocities v of the particle, namely,[4,5]

$$P^+ = (2/\pi)\exp[-(\pi/2\gamma v)(I - \phi - \delta_{ic})], \qquad (4)$$

where $\phi = 4.4$ eV is the work function of Al(100), $I = 6$ eV is the ionization energy of an Al atom, and $\delta_{ic} = 0.68$ eV is the image charge correction corresponding to a distance of 10 a.u. from the surface. In order to compare Eq. (4) quantitatively with experiments, it would be essential to average Eq. (4) over various values of $I-\phi$ in the exponent of Eq. (4) because they vary for different surface charges in different cascades. However, the magnitude and statistical distribution of $I-\phi$ is currently unknown so that we can make only rough estimates.

For 5 eV Al emitted along the surface normal, the perpendicular velocity v is 0.0027 a.u. and P^+ in the unperturbed solid would be 5×10^{-18}. In order to obtain the experimental value of $P^+ = 5 \times 10^{-4}$, the energy difference 0.92 eV in the exponent of Eq. (4) would have to be reduced to 0.18 eV by an external potential. It is unlikely, however, that any local charge imbalance at the surface of Al would cause a change of 0.74 eV at a distance of 10 a.u. from the surface. Moreover, similar enhancements of P^+ have been seen, e.g., in Cu (Ref. 14) or in Ag (Ref. 15), which have still higher ionization energies that would require changes of the potential above the surface to be around 2–3 eV.

B. Thermalized excitation models of ionization and neutralization

In view of this observation, we instead assume that the main reason for the enhancement of the charge transfer in multiple scattering and sputtering is electron-hole excitation in the substrate, rather than induced quasistatic electric dipoles on the surface. The basic assumption of this excitation model is that the electron-hole diffusion length in a locally heavily electronically excited metal is much shorter than in the unperturbed metal. To illustrate this point, we will apply the excitation model to the situations shown in Figs. 1 and 2.

As the trajectories of all atoms in Figs. 1 and 2 are well known, it is straightforward to calculate the electronic energy density $E(\mathbf{r},t)$ transferred from the moving atoms into the system. As discussed, e.g., in Ref. 15, the time-space development of $E(\mathbf{r},t)$ can be described by the diffusion equation

$$\frac{\partial E(\mathbf{r},t)}{\partial t} - D\nabla^2 E(\mathbf{r},t) = A\sum_i E_k^i(t) \cdot \delta(\mathbf{r}_i - \mathbf{r}), \qquad (5)$$

where D is the diffusion constant and A is the constant in the source term discussed in detail in Ref. 15. The value of A is 9.2×10^{-5}(a.u.) for Cu in Cu metal. E_k^i is the kinetic energy of the ith particle in the cluster. The summation on the right side of Eq. (5) is over all particles in the cluster. The value D is assumed to depend only on time, and the excitation is allowed to spread over the whole space and not only inside the cluster. Computer experiments show that both these approximations only slightly influence the value of $E(\mathbf{r},t)$ at the surface of the cluster. Once $E(\mathbf{r},t)$ is known, it can be converted into the electronic temperature T_e using the rela-
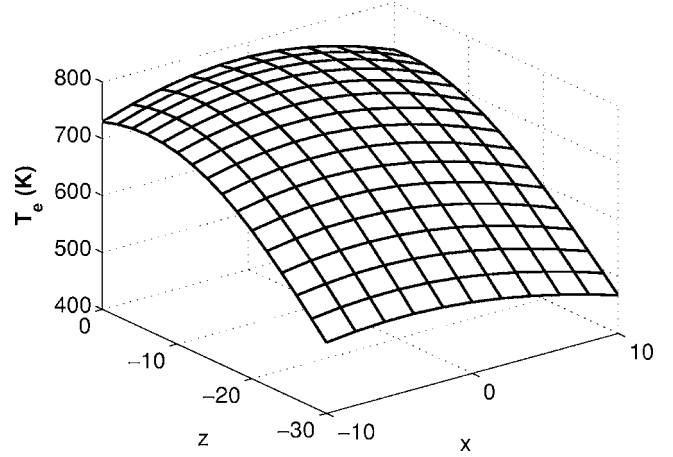

FIG. 3. The distribution of the electronic temperature $T_e(\mathbf{r},t)$ at the (001) surface ($z=0$) of the cluster of Cu atoms in the situation shown in Fig. 2 at the time when the Na$^+$ ion is neutralized ($t=5000$ a.u.). The values of $T_e(\mathbf{r},t)$ are calculated using the diffusion equation (5) with $D=1$ a.u. (equivalent to $D=1.16$ cm^2 s^{-1}) and using the electronic heat capacity of the free electron gas.

tion $T_e(\mathbf{r},t) = [(2/C)E(\mathbf{r},t)]^{1/2}$, where C is the electronic specific heat divided by T_e, and has a value of $C=2.1 \times 10^{-12}$(a.u./K) for Cu.

The dependence of D upon the time interval after the impact of the particle is not known from theoretical estimates, but fitting to experiments[15] indicates that D varies from values above $D=100$ a.u. in unperturbed solids to about $D=1$ a.u. (corresponds to 1.16 cm^2 s^{-1}) in a heavily perturbed solid. The value $D=1$ a.u. corresponds to a mean-free path that is equal to interatomic distances in typical metals. In the single-scattering trajectory shown in Fig. 1, the time when the particle is neutralized is rather short (25 fs) and D can be still quite large. Even with D as small as 5 a.u., the effect of the excitation is small and the neutralization is still a fully nonadiabatic process as confirmed by experiments. Similar timing and thus similar values of N_p occur not only in single-scattering experiments, but also for particular multiple-scattering trajectories when the particle slides over the surface [see Figs. 2(b)–2(d) in Ref. 11] and does not penetrate into the solid.

If the particle penetrates deeper into the substrate as in Fig. 2, however, the neutralization process occurs 100 fs after the impact of Na. Because a longer time elapsed after the impact, more electronic energy is transferred into the substrate and D may decrease to 1 a.u.. Using Eq. (4) and $D=1$ a.u., we have calculated $E(\mathbf{r},t)$ and $T_e(\mathbf{r},t)$ at the time of the neutralization at the surface of the cluster. The resulting space distribution of T_e at the time of neutralization is shown in Fig. 3. If the calculated average value of the surface $T_e=850$ K is substituted into Eq. (1), we obtain $N_p=0.23$, which is closer but still smaller than the experimental value of N_p. In fact, if the neutralization is mainly due to thermal excitations, then the use of the simple Fermi distribution is not justified and the spin-orbital degeneracy of the neutral and ionized atoms must be taken into account. Because neutral Na is twice spin-degenerate, the actual neutralization is twice as large, i.e., $N_p=0.46$, which is in good

agreement with the experiment. The very large values of $N_p(>0.6)$ observed for multiply-scattered Na during the 400 eV Na scattering shown in Fig. 2 in Ref. 1 can also be consistently described within the same picture. The value of T_e calculated from Eq. (5) for a 400 eV impact with $D=1$ a.u. is 1500 K, i.e., considerably higher than the 850 K calculated for a 50 eV impact.

According to the electronic excitation model discussed above, particles singly scattered (or directly recoiled[13]) from metal surfaces are neutralized (or ionized) by purely nonadiabatic processes because there is not enough time (<25 fs) to develop a sufficient concentration of e-h pairs in the substrate. Multiply scattered or sputtered particles are, on the other hand, neutralized (or ionized) by adiabatic processes in which the e-h pairs in the substrate play an essential role and the parameter T_e represents their actual temperature. Formula (4) can then be replaced by

$$P^+ = \left(\frac{Z^+}{Z^0}\right)\exp\left[-\left(\frac{1}{kT_e}\right)(I - \phi - \delta_{ic})\right], \qquad (6)$$

where Z^+ and Z^0 are the partition functions of emitted ions and neutrals at T_e. The other parameters are the same as in Eq. (4). It should be stressed that the validity of Eq. (6) depends upon the condition $kT_e \gg \gamma v$. In turn, a sufficiently high T_e can develop only if the electron mean-free path in the cascades is of the order of interatomic distances, as assumed in the above analysis.

The assumption of high electronic temperatures in collision cascades explains the characteristic strong enhancement of ionization of low-energy sputtered particles in a natural, and even quantitative, manner.[13,15] The low-energy (typically below 20 eV) particles are the most abundant in sputtering. This enhancement is difficult to explain in terms of one-electron nonadiabatic processes, as pointed out in the previous section. The nonadiabatic processes become prevailing, however, in the ionization of less abundant high-energy sputtered particles, which are often referred to as direct recoils.[13,16] We should mention that the mechanisms of ionization and neutralization, described in this paper, are applicable generally for metal and semiconducting substrates. For ionic substrates with large band gaps, the "bond breaking" model, analogous to an ion-pair dissociation in the gas phase, has been found to be appropriate.[17]

III. ELECTRON EMISSION FROM METALS INDUCED BY THE IMPACT OF METAL IONS

Kinetic electron emission (KEE) produced by the impact of slow metal particles on metal surfaces can, to some extent, be related to the ion formation processes described in the previous section. Provided that only valence electrons near the metal Fermi level are excited, similar matrix elements are involved in both processes. However, the timing is different, as KEE occurs within a few fs after the impact and, as compared to ion neutralization, the emission may originate from considerably deeper below the surface. It is thus conceivable that other processes contribute to KEE. It should be stressed that despite a considerable effort, the microscopic mecha-

nism of KEE has not been identified in most cases, particularly at very low impact energies, in contrast to the well-understood potential electron emission (PEE).[18] At higher impact energies, electron promotion,[19] plasmon assisted emission processes,[20] and direct particle-electron collisions[21] may all contribute to KEE. These processes, however, have well-defined thresholds in the impact energy of the atomic projectile, below which their contribution to the emission decreases rapidly.[22] Nevertheless, even below the thresholds, the magnitude of the observed KEE is usually quite strong. Electron emission from metals induced by the impact of metal ions is particularly suitable for studies of this sub-threshold region because the electronic structure of the projectile-substrate system excludes PEE.

Relevant experimental studies of KEE investigated the emission induced by the impact of Na$^+$ ions on a Ru metal surface. These experiments, together with a tentative interpretation, were published in Ref. 23. Similar studies with nonmetallic projectiles impinging upon a Au surface had been published previously in Ref. 24. In these experiments, any contribution of PEE could be excluded, and promotion, plasmon, and direct particle-electron collision processes play only a minor role.

A. Nonadiabatic models of the subthreshold KEE

In the theoretical description, parameters $V_{kk'}(t)$ have been used,[23,24] which represent the transfer matrix elements of the perturbing particle potential between the metal conduction k states. Provided that the amplitude and time dependence of these matrix elements are known, the total number of electrons Γ emitted into the vacuum within a solid angle $d\Omega$ is given in the first order perturbation by the nonadiabatic process,[23,24] such that

$$\Gamma = 2(d\Omega/4\pi)\int_\phi^\infty d\varepsilon \cdot \rho(\varepsilon)T_r(\varepsilon)\int_{-\infty}^0 d\varepsilon' \cdot \rho(\varepsilon')$$

$$\times \left|\int_{-\infty}^{+\infty} dt[V_{kk'}(t)]\exp\{i(\varepsilon - \varepsilon')t\}\right|^2, \qquad (7)$$

where $\rho(\varepsilon)$ is the electron density of the metal at the energy ε, and ϕ is the work function of the metal surface. The Fermi energy ε_f was set to zero. $T_r(\varepsilon)$ describes the surface transmission function.[18] The factor of 2 is due to the spin degeneracy.

In order to make further analysis feasible, we use similar approximations as those used in the derivation of Eq. (1).[4,5] Namely, it is assumed that $\rho(\varepsilon)$ is a constant equal to $\rho=\rho(\varepsilon_f)$ and all of the $V_{kk'}$ terms are the same and equal to $V(t)$. Since the main purpose of the following analysis is a comparison of the efficiencies of various excitation processes, we will calculate and compare the total number of electrons excited above the vacuum level in the upper space hemisphere. Thus in Eq. (7), we set $T_r(\varepsilon)=1$ and $2(d\Omega/4\pi)=1$. Equation (7) then simplifies to

$$\Gamma = \rho^2\int_\phi^\infty d\varepsilon\int_{-\infty}^0 d\varepsilon' \left|\int_{-\infty}^{+\infty} dt[V(t)]\exp\{i(\varepsilon - \varepsilon')t\}\right|^2.$$
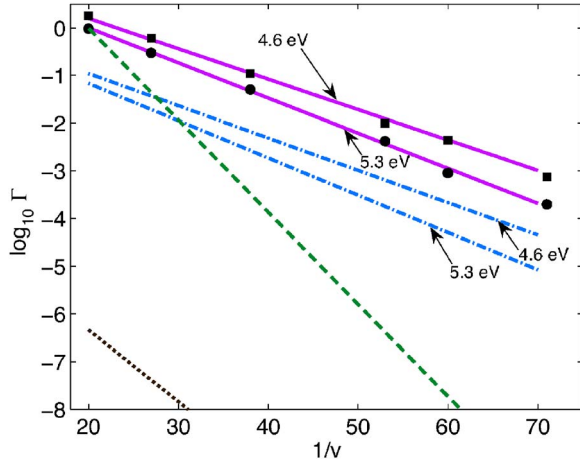
$$(8)$$

FIG. 4. (Color online) The electron yield Γ as a function of the inverse velocity of Na$^+$ impinging perpendicularly upon the Ru(0001) surface is shown by solid black dots for ϕ=5.3 eV and by solid squares for ϕ=4.6 eV.[23] Only electrons emitted along the surface normal were collected and the value of Γ was approximately estimated from the angular acceptance of the spectrometer. The yields predicted by the nonadiabatic model (9) with γ=1.8 a.u. (also discussed in Ref. 23) are shown by the solid lines for the two ϕ's and by the dashed lines for a realistic γ=0.687 and ϕ=5.3 eV. The preexponential factors were adjusted to fit the experiment at v^{-1}=20. The yield predicted by the model (12) with the parameters taken from the scattering data is shown by the dotted line for ϕ =5.3 eV. The yields predicted from the hot-spot model (13) are marked by the dashed-dotted lines for both ϕ's.

Because of the approximate form of the interaction potential and the density of states, the model is not suitable for studies of the angular dependences of KEE. We will assume, as was done in relevant experiments,[23,24] that the bombarding particle approaches the surface in the normal direction with velocity v, and passes the surface at $z=0$ without significant attenuation. We will further assume that the z dependence of $V(z)$ follows the z dependence of the conduction electron density at the Fermi level. In vacuum far away from the surface, the value of V typically decays as $V \exp(-2\gamma z)$, where $(2\gamma)^{-1}$ is the decay length of the electron density at the Fermi level. Because $z=vt$, the value of V is time dependent. Once $V(t)$ is known, the value of Γ can be obtained from Eq. (8).

We have chosen three model forms of $V(z)$ which resemble the expected shape of the particle-electron interaction at the surface. They all decay as $V \exp(-2\gamma z)$ for large positive z. The corresponding Γ's have analytical forms if $\gamma v \ll \phi$ (which is practically always the case) and are shown below for each V,

$$V(z) = V/\cosh(2\gamma z), \quad \Gamma = 4\rho^2 V^2 \exp[-(\pi/2\gamma v)\phi], \quad (9)$$

$$V(z) = (V/2)[1 - \tanh(\gamma z)], \quad \Gamma = 4\rho^2 V^2 \exp[-(\pi/\gamma v)\phi], \quad (10)$$

$$V(z) = (V/2)[1 - \tanh(\gamma z)][\cos(k_f z)]^2, \quad \Gamma = R^2 4\rho^2 V^2 \exp[-(\pi/\gamma v)\phi]. \quad (11)$$

The first relation, Eq. (9), describes a perturbation of the

amplitude V that is localized at the surface within a distance of about $(2\gamma)^{-1}$. Relations (10) and (11) describe true surface perturbations that increase from 0 to V at the surface within a distance on the order of $(2\gamma)^{-1}$, and k_f is the Fermi wave vector of the substrate. The most realistic of these is relation (11), which includes the interaction with electrons in the bulk, equivalent to the classical electron-particle collision process.[25] We assume that the oscillatory term is nonzero only within the distance of the mean-free path (10 a.u.) from the surface. The value of the preexponential factor R depends upon the ratio k_f/γ, specifically $R=1$ if $k_f < \gamma$, $R=5$ if $k_f=\gamma$, $R=15$ if $k_f=1.4\gamma$, $R=50$ if $k_f=1.8\gamma$, and $R=100$ if $k_f=2\gamma$. However, the slopes of Γ do not change.

We will also consider the excitation induced by electron transfer from the projectile orbital into the metal orbitals. This resonant transfer is responsible for the ion formation and neutralization as discussed in the previous section and described by Eq. (1). The same resonance transfer process can also lead to electron emission and the effective perturbing potential $V(z)$ for KEE can be expressed in terms of the virtual line width $\Delta(z)$ and the shift $\delta\varepsilon(z)$ of the projectile valence orbital.[22,26] For the Na-jellium system, these parameters are known quantitatively and are given in the previous section by Eqs. (2) and (3). The potential $V(z)$ and the corresponding Γ are then given by

$$V(z) = (1/\rho\pi)\left(\frac{\Delta(z)}{[i\Delta(z) + \varepsilon' - \delta\varepsilon(z)]}\right),$$

$$\Gamma = 0.00048 \exp[-(\pi/1.78v)\phi]. \quad (12)$$

In all four cases [Eqs. (9)–(12)], the value of Γ depends exponentially upon v^{-1} and ϕ. In order to compare the theoretical predictions quantitatively, the experimental dependence of Γ on v^{-1}, induced by the impact of Na on Ru(0001), is reproduced in Fig. 4 from Ref. 23 by black dots and triangles for two different Ru work functions. The most conspicuous and reproducible aspect of the experiment is the exponential dependence of Γ on v^{-1} and ϕ, in agreement with the prediction of Eqs. (9)–(12). The absolute magnitude of Γ is less well known due to the uncertainties in the determination of experimental collection efficiency. We have estimated from the geometry of our setup that Γ is about 1 for v^{-1}=20 a.u. (this value corresponds to 1400 eV Na).

In Eqs. (9)–(11) the value of γ is expected to be close to the value of k_f of Ru, which is 0.687 a.u. The graph of Γ as a function of v^{-1} calculated from Eq. (9), with γ=0.687 and ϕ=5.3 eV, is shown in Fig. 4 by a dashed line. The preexponential factor $4\rho^2 V^2$ is set equal to 7375 in order to fit the expected absolute value of Γ. It is obvious from the graph, however, that the (negative) slope of the calculated Γ is much steeper than the experimental slope. Moreover, if we assume that V is localized within the atomic volume, the value of V would be much too large (above 100 eV). The other model potentials, Eqs. (10) and (11), also do not improve the results. Because exponents of Γ in Eqs. (10) and (11) depend on γ and not on 2γ, as in Eq. (9), the slopes are even steeper. The potential (12), which is deduced from the resonance charge process and which has no adjustable pa-

rameters to correct the absolute value, leads to the Γ shown by the dotted line. Although the slope is less steep, it is still steeper than the experimental slope and the amplitude is far too small.

The semiphenomenological model (9) describes all characteristic features of the experiment very well when γ is taken equal to 1.8, as illustrated in Ref. 23. The resulting Γ is shown in Fig. 4 by full lines for $\phi=5.3$ eV and $\phi=4.6$ eV and with the preexponential factor $4\rho^2 V^2$ set equal to 30. The agreement with experiment is good, the amplitude of the potential V is reasonable (about 3 eV), but the space dependence of V, given by $\gamma=1.8$, is much too small for valence orbitals of Na and valence metal electrons. The range of the electronic interaction $(2\gamma)^{-1}$ would be only 0.27 a.u., which is too small for extended valence orbitals. One possible explanation is that the more compact inner shell orbitals are admixed into valence bands by orthogonalization processes and thus the effective value of γ is increased. One would expect that the effective value γ would then be a function of the impact energy of Na$^+$ as the projectile penetrates deeper into the substrate atom. Experimentally, however, this it is not the case and the value of γ remains the same within the whole range of Na$^+$ impact energies that were studied, i.e., from 120 to 1600 eV. Another possibility, as suggested in Ref. 23, is the effect of the electron-electron interactions in the impact zone which, without changing the energy losses, broaden the electron energy distribution and effectively increase the value of γ.

B. Thermalized excitation models of KEE

The difficulties in interpreting KEE in terms of one-electron excitation points out that the electron emission could be a more complex many-electron process where electron-electron interactions play an important role. Because there is a lack of any comprehensive many-electron theory of the excitation induced by an atomic particle passing through the electron gas, we will use a simplified thermal hot-spot model for illustration purposes. The model can be again based on the diffusion equation (5). The emission process, however, occurs in such a short time that the concept of electron-hole pair diffusion is questionable and its time-space dependence is not known.

In this simple semiclassical model, we assume that the excitation occurs in an interval $\delta t=50$ a.u., which is short enough to keep the excitation localized and long enough to allow electrons to interact and to come closer to thermal equilibrium. The localization is assumed to be within the interatomic distance $r=5$ a.u. In this volume, the e-h pair interaction is not yet fully screened. After each δt, the excitation is completely delocalized and a new excitation takes place in the next δt. The energy transferred during δt into the electron gas from the particle moving with kinetic energy E_k is, as assumed in Eq. (5), equal to $A E_k \delta t$. The corresponding energy density within the excited volume is $A E_k \delta t/(4\pi r^3/3)$ and the corresponding electron temperature $T_e=(2/C)^{1/2}(A E_k \delta t)^{1/2}(4\pi r^3/3)^{-1/2}=Bv/k$, where v is the velocity of the projectile, k is the Boltzmann constant, and B has a constant value for a given particle and substrate.

It is assumed that the electrons can be emitted from within the substrate up to a depth equal to the escape length λ so that the number of the time intervals δt during the complete emission process is equal to $\lambda/(v\,\delta t)$. The yield Γ of electrons emitted above the vacuum level in the upper half of the space is then

$$\Gamma = \rho\left(\frac{\lambda}{v\,\delta t}\right)\int_0^\infty d\varepsilon\,\exp\left[\frac{-(\varepsilon+\phi)}{kT_e}\right] = \rho\left(\frac{\lambda}{v\,\delta t}\right)kT_e\exp\left[\frac{-\phi}{kT_e}\right]$$
$$= \rho\left(\frac{\lambda B}{\delta t}\right)\exp\left[\frac{-\phi}{Bv}\right], \qquad (13)$$

where ρ is the density of states as used before and ε is set to zero at ϕ. It should be stressed that the velocity v in Eq. (13) is not necessarily the perpendicular component of the projectile velocity as it is for the surface potentials (10)–(12).

The values of A and C that correspond to a Na projectile and a Ru target are not accurately known. As there is no experimental evidence that electron yields are much different for different metallic substrates and projectiles[24] we take A and C, for simplicity, from the Na–Cu system, namely $A=6\times 10^{-5}$ a.u. and $C=2.1\times 10^{-12}$(a.u./K). The electronic temperature is then $T_e=4500$ K for 100 eV Na impact and increases to $T_e=14\,000$ K for 1000 eV Na. In Fig. 4, we show the electron yields calculated from Eq. (13) as a function of v^{-1} by the dashed-dotted lines for both values of the work function. The agreement with the experiment is reasonably good. Although it systematically underestimates the experimental yield, the slopes of the curves and the relative positions of the $\phi=4.6$ and 5.3 eV are correct. The energy dependence of the electrons emitted with the energy ε is given by the exponential dependence $\exp(-\varepsilon/kT_e)$, which is also in a very good agreement with experimental data in Ref. 23 over the whole range of impact velocities. The relation (13) predicts an increase of Γ with the angle of incidence because the electrons are excited closer to the surface so that the effective escape depth is larger.

Although the hot-spot model presented here is heuristic and without a firm theoretical background, it currently represents the only possible semiquantitative description of many-particle processes in KEE. The agreement of Eq. (13) with experiments for a reasonable choice of parameters is not fortuitous, but indicates that the hot-spot model may indeed closely describe the many-particle nature of KEE from bombarded metals.

IV. CONCLUSIONS

We have analyzed ionization and neutralization of metallic atoms emitted from metal substrates in terms of nonadiabatic and adiabatic electron transfer processes. We confirmed that charge exchange of singly scattered metal atoms is determined by a nonadiabatic process that can be characterized by a few well-defined time-dependent parameters of the particle-surface interaction, while the excited electron-hole pairs in the substrate can be neglected. If the particle is emitted after multiple scattering or sputtering, however, the substrate becomes strongly dynamically perturbed at the time of

emission. This perturbation can lead to substrate *e-h* excitations that are partially localized in the region of the perturbation, which can be characterized by a local electronic temperature T_e. The excited electrons and holes transport adiabatically to and from the emitted particle, and this transport, rather than a nonadiabatic electron transfer, may determine its charge. The localization of the excitation is an essential assumption in the model and is described in a phenomenological way with a small electron-hole transport diffusion constant. We estimated the value of T_e numerically for well-defined trajectories of Na scattered from Cu(001), and used these values to calculate the neutralization probability of multiply scattered atoms and found a reasonable agreement with experiment. This approach is more appropriate in explaining the large increase of the atom-surface charge exchange that is experimentally observed for perturbed surfaces than is the alternative approach that assumes quasistatic charge imbalance and the ensuing quasistatic random electrostatic fields on such surfaces.

The interaction of slow metallic particles with metal surfaces also leads to KEE. At sufficiently low impact energies, KEE is due only to valence electron transfer so that excitations and other KEE mechanisms, such as electron promotion of deep levels, can be excluded. We have analyzed in detail a mechanism, based on particle-surface valence electron transfer, which is a direct analogue of ion formation for which all matrix elements are known from scattering experiments. For a Na$^+$ projectile, however, this process gives KEE yields that are much too small to explain the experimental observations. The nonadiabatic process based on a rapid passage of the particle through the surface potential would give results in good agreement with the experiment, but the surface interaction region must be chosen to be unrealistically narrow (0.25 a.u.) for a valence electron transfer interaction. We have made an attempt to describe KEE in terms of a "hot-spot model." The agreement with the experiment is good if we assume that the excited *e-h* pairs are localized, for at least 10^{-15} s in a region of approximately 5 a.u. in diameter, in which electron-electron interactions are not yet heavily screened.

*Corresponding author. Email address: yarmoff@ucr.edu.

[1] G. A. Kimmel and B. H. Cooper, Phys. Rev. B **48**, 12164 (1993).

[2] C. E. Sosolik, J. R. Hampton, A. C. Lavery, B. H. Cooper, and J. B. Marston, Phys. Rev. Lett. **90**, 013201 (2003).

[3] C. B. Weare and J. A. Yarmoff, Surf. Sci. **348**, 359 (1996).

[4] W. Bloss and D. Hone, Surf. Sci. **72**, 277 (1978).

[5] R. Brako and D. M. Newns, Surf. Sci. **108**, 253 (1981).

[6] J. B. Marston, D. R. Andersson, E. R. Behringer, B. H. Cooper, C. A. DiRubio, G. A. Kimmel, and C. Richardson, Phys. Rev. B **48**, 7809 (1993).

[7] P. Nordlander and J. C. Tully, Phys. Rev. Lett. **61**, 990 (1988).

[8] P. Nordlander and J. C. Tully, Phys. Rev. B **42**, 5564 (1990).

[9] E. Runge and E. K. U. Gross, Phys. Rev. Lett. **52**, 997 (1984).

[10] E. R. Behringer, D. R. Andersson, B. H. Cooper, and J. B. Marston, Phys. Rev. B **54**, 14765 (1996).

[11] C. A. Keller, C. A. DiRubio, G. A. Kimmel, and B. H. Cooper, Phys. Rev. Lett. **75**, 1654 (1995).

[12] G. Betz, M. J. Pellin, J. W. Burnett, and D. M. Gruen, Nucl. Instrum. Methods Phys. Res. B **58**, 429 (1991).

[13] X. Chen, Z. Sroubek, and J. A. Yarmoff, Phys. Rev. B **71**, 245412 (2005).

[14] D. V. Klushin, M. Y. Gusev, S. A. Lysenko, and I. F. Urazgil'din, Phys. Rev. B **54**, 7062 (1996).

[15] A. Duvenbeck, F. Sroubek, Z. Sroubek, and A. Wucher, Nucl. Instrum. Methods Phys. Res. B **225**, 464 (2004).

[16] D. V. Klushin, M. Y. Gusev, and I. F. Urazgil'din, Nucl. Instrum. Methods Phys. Res. B **100**, 316 (1995).

[17] P. Williams, Surf. Sci. **90**, 588 (1979).

[18] R. A. Baragiola, in *Low Energy Ion-Surface Interactions*, edited by J. W. Rabalais (Wiley, New York, 1994).

[19] M. Barat and W. Litchen, Phys. Rev. A **6**, 211 (1972).

[20] P. Riccardi, P. Barone, A. Bonanno, A. Oliva, and R. A. Baragiola, Phys. Rev. Lett. **84**, 378 (2000).

[21] H. Winter and HP. Winter, Europhys. Lett. **62**, 739 (2003).

[22] Z. Sroubek and J. Fine, Phys. Rev. B **51**, 5635 (1995).

[23] J. A. Yarmoff, H. T. Than, and Z. Sroubek, Phys. Rev. B **65**, 205412 (2002).

[24] J. Lörincik, Z. Sroubek, H. Eder, F. Aumayr, and HP. Winter, Phys. Rev. B **62**, 16116 (2000).

[25] G. Falcone and Z. Sroubek, Phys. Rev. B **39**, 1999 (1989).

[26] J. A. Yarmoff, T. D. Liu, S. R. Qiu, and Z. Sroubek, Phys. Rev. Lett. **80**, 2469 (1998).